Proceedings of the 11th Brazilian Congress of Thermal Sciences and Engineering -- ENCIT 2006
Braz. Soc. of Mechanical Sciences and Engineering -- ABCM, Curitiba, Brazil, Dec. 5-8, 2006

Paper CIT06-0353

NUMERICAL SOLUTION OF ONE-DIMENSIONAL REACTIVE FLOWS IN ROCKET ENGINES WITH REGENERATIVE COOLING

Luciano Kiyoshi Araki
Programa de Pós-graduação em Métodos Numéricos em Engenharia, UFPR, Curitiba, PR, Brazil
lucaraki@demec.ufpr.br

Carlos Henrique Marchi
Departamento de Engenharia Mecânica, Universidade Federal do Paraná, Curitiba, PR, Brazil
marchi@demec.ufpr.br

Abstract. *The maximum temperature in the internal structure and the pressure drop on the coolant flow along the channels are two of the most important design parameters for rocket engines with regenerative cooling. A one-dimensional mathematical model for the reactive flows in a LOX/LH_2-rocket engine with regenerative cooling is presented. This problem includes the combustion gases flow in the rocket diverging-converging nozzle, the coolant flow in channels and the heat transfer through the walls (from combustion gases to coolant). For the combustion gases flow, three different physical flow models are used: a frozen, an equilibrium and a non-equilibrium one. Several chemical reaction schemes are also taken into account for each study, for the evaluation of effects of the species and reaction equation systems on the final numerical solution. Besides the influence of physical and chemical models on the answers, the effects of the adopted grids over the final results are also discussed. Therefore numerical errors estimative are also made and the physical and chemical models results are compared. Numerical results are obtained with a finite volume software, implemented with second order scheme for variables, co-located grid arrangement for all speed flows and Fortran 95 language.*

Keywords. *Finite volume method, CFD, equilibrium flow, non-equilibrium flow, numerical error estimate.*

1. Introduction

The thrust chamber is the key subassembly of a rocket engine, where the liquid propellants are metered, injected, atomized, vaporized, mixed and burnt, to form hot reaction gas products (Sutton and Biblarz, 2001). By speeding up these gases, thrust force is obtained for orbit and payload definition. The knowledge of chemical and physical phenomena concerned about such gases flow is, therefore, important for both rocket design (associated to material definition and cooling system design) and mission goals achievement.

Heat is transmitted to all internal hardware surfaces exposed to hot gases, namely the injector face, the chamber and nozzle walls. Only 0.5 to 5% of the total energy generated in the gas is transferred as heat to the chamber walls (Sutton and Biblarz, 2001). This amount of energy, however, can increase the wall temperatures until material failure. Because of this, most of rocket engines have cooling systems, which allow a longer lifetime for the entire device. One of the most used cooling systems for large rocket engines is the regenerative one. The prediction of heat transfer characteristics in a regeneratively cooled rocket combustion engine is one of the most important and most challenging tasks in the design work of a high performance engine (Fröhlich *et al*., 1993).

The problem involving reaction gas products flow and heat transfer to cooling system may be divided up into three sub-problems, namely: the reactive combustion gases flow through the thrust chamber (which includes the combustion chamber and the nozzle engine); the heat conduction from hot gases to the coolant, through the wall structure; and the turbulent coolant flow, in the regenerative cooling system. The solution for the whole problem can be obtained by solving, iteratively and in sequence, the three sub-problems, allowing them to interact, until its convergence.

Although two and three-dimensional models are commonly used, one-dimensional models are still employed in rocket engines projects, being corrected by empirical coefficients (Fröhlich *et al*., 1993; Sutton and Biblarz, 2001). Studies involving one-dimensional softwares are, because of this, still useful. Based on this, in this work an one-dimensional model, which includes different physical and chemical schemes, is purposed for solving the coupled problem of reaction gas products flow and heat transfer to the thrust chamber structure and coolant.

Four physical models (one-species with variable properties, frozen, local equilibrium and non-equilibrium flows) are studied. Both frozen and local equilibrium flows are ideal models; they differ, however, about how the chemical reactions take place during the flow. For both frozen and local equilibrium physical models, nine different chemical reaction schemes are used. These schemes are the same presented before by Marchi *et al*. (2005), and include from three to eight chemical species and take into account from null to eighteen chemical reaction equations. For non-equilibrium model, five different chemical schemes are used, including six or eight chemical species, which totalise five chemical schemes. At this work, however, only two chemical models are studied (one six-species and one eight-species for frozen and equilibrium flows and two six-species for non-equilibrium flow). According to Marchi *et al*. (2005) and Araki and Marchi (2006), six and eight-species models present good accuracy with CEA results (Glenn Research

Center/NASA, 2005), for frozen and equilibrium flows with adiabatic walls, reason for considering only six and eight-species models in this work.

All the models have been implemented using Compaq Visual Fortran 6.6.0. The implemented software, called RHG1D 3.0, was run at a PC Pentium IV, 3.4 GHz, with 4 GB RAM. Results are compared to those ones obtained for adiabatic walls simulations and numerical error estimates, related to all the results and based on GCI estimative (Roache, 1994), are also presented.

2. Mathematical model

The basic principles of the rocket propulsion are essentially those of mechanics, thermodynamics and chemistry (Sutton and Biblarz, 2001). The flow and heat transfer problem in rocket thrust chambers can be divided up into three different (but coupled) problems, for which there are independent mathematical (and numerical) models: (1) the reaction gas products (combustion gases mixture) flow through the thrust chamber; (2) the heat conduction from hot gases to the coolant; and (3) the coolant flow through the regenerative cooling system. Figure 1 shows, schematically, both the reaction gas products and the coolant flows.

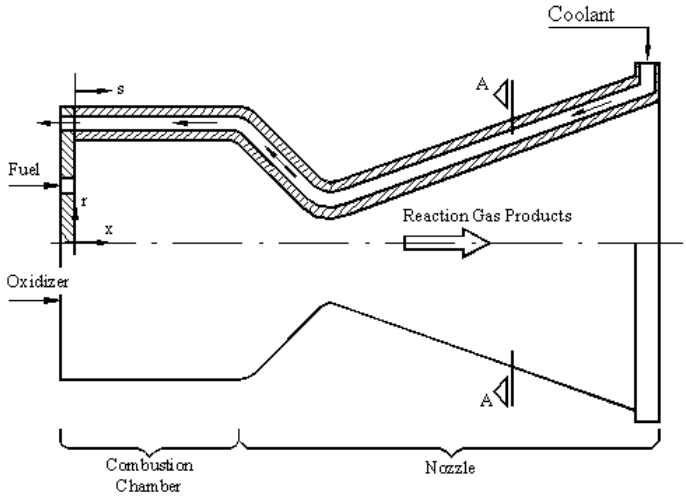

Figure 1.Thrust chamber engine with regenerative cooling system (transversal section).

2.1. Reaction gas products flow

The mathematical formulation for a one-dimensional, single-species flow (or a multi-species frozen or equilibrium flow) through the nozzle engine is based only on four equations: conservation of mass, conservation of momentum, conservation of energy and state (the one-species gas and/or the multi-species gas are treated by the perfect gases law), given in the sequence:

$$\frac{d}{dx}(\rho u S) = 0\,, \tag{1}$$

$$\frac{d}{dx}(\rho u S u) = -S\frac{dP}{dx} + F'\,, \tag{2}$$

$$c_p \frac{d}{dx}(\rho u S T) = u S\frac{dP}{dx} + q' + S_{eq/ne}\,, \tag{3}$$

$$P = \rho R T\,, \tag{4}$$

where: ρ, u, P and T are four dependent variables, related to density, velocity, pressure and temperature (in this order); x is the axial coordinate along the gases flow (Fig. 1); S is the internal cross-sectional area of thrust chamber structure; R is the gas constant (or gas mixture constant, for frozen and equilibrium flows); c_p is the constant-pressure specific heat; F', q' and $S_{eq/ne}$ are related to the viscous forces, the heat loss to the walls and the source term correspondent to equilibrium or non-equilibrium conditions (this term is necessary only for equilibrium or non-equilibrium flows), respectively, and are evaluated by the following relations:

$$F' = -\frac{\pi}{8} f\, \rho u \left| u \right| D, \tag{5}$$

$$q' = \left| u\, F' \right| + S'_{wall}\left(q''_h + q''_r\right), \tag{6}$$

$$S_{eq/ne} = \begin{cases} -\sum_{i=1}^{N} h_i \frac{d}{dx}\left(\rho\, u\, S\, Y_i\right), & \text{for local equilibrium flow;} \\ -S\sum_{i=1}^{N} h_i \dot{w}_i, & \text{for non-equilibrium flow;} \end{cases} \tag{7}$$

where: f is the Darcy friction factor; D is the diameter of the cross-section; S'_{wall} is the internal wall surface by length unity (along x-axis, Fig. 2); N is the total number of species existent in the flow; h_i is the enthalpy for each chemical species i; Y_i is the mass fraction for each chemical species i; $\dot{w}_i$ corresponds to mass rate generation of species i; and q''_h and q''_r are the convection and radiation heat fluxes to internal walls.

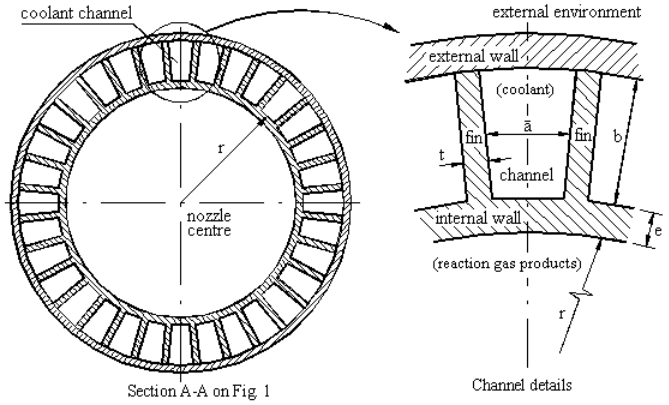

Figure 2. Cooling channels and their geometrical parameters.

As can be seen previously, the conservation of energy, Eq.(3), has the temperature as unknown and not the enthalpy nor the internal energy, as normally used. The major advantage of such variation is about the temperature determination, which can be obtained directly from the numerical model, not depending on the enthalpy (or internal energy) values. Besides the gas products flow, chemical reaction schemes have an important role on final results. Frozen, equilibrium and non-equilibrium models, in different levels, take into account chemical reactions. Depending on the adopted chemical reaction scheme, different chemical composition and physical properties are obtained or, at least, larger or smaller CPU time efforts are verified. For the frozen model, by hypothesis, the flow from combustion chamber to thrust chamber exit is so fast that there is no time for changes in chemical composition of reaction gas products. For the local equilibrium model, in counterpart, chemical equilibrium composition must be evaluated for every single cross-section of the thrust chamber. An intermediate (and more realistic) model between local equilibrium and frozen ones is the non-equilibrium. For this model, chemical composition must be evaluated for every single cross-section of the thrust chamber as done for local equilibrium; the equilibrium composition, however, is not reached and, for each single chemical species, mass formation rates are evaluated.

For frozen and equilibrium models, nine different chemical reaction schemes were implemented, taking into account from 3 to 8 chemical species and from null to eighteen chemical reaction equations, as can be seen at Table 1 where N is the number of chemical species and L is the number of chemical reaction equations. Chemical reaction schemes implemented in software Mach1D 5.0, for both frozen and local equilibrium flows, are the same presented by Marchi *et al*. (2005). For non-equilibrium flow, only six and eight-species models were considered, totalising five. For both frozen and equilibrium flows, different chemical schemes mean at least one different chemical reaction equation (even when the same number of chemical species and the same number of chemical reaction equations are considered). For non-equilibrium, otherwise, different chemical schemes mean, at least, different forward reaction constant: based on this, model 3 could be split up into two ones (the other non-equilibrium models are 5, 7 and 10).

At non-equilibrium flow model, forward and backward reaction constants (kf_j and kb_j, respectively) have an important role for mass generation rates evaluation, being related to each other by the progression rate of reaction j (γ):

$$\gamma_j = \left\{ kf_j \prod_{i=1}^{N} C_i^{\nu'_{ij}} - kb_j \prod_{i=1}^{N} C_i^{\nu''_{ij}} \right\}, \tag{8}$$

where C_i is the molar concentration of species i in gases mixture and ν'_{ij} and ν''_{ij} are, in this order, the stoichiometric coefficients of chemical species i in reaction j existent in reagents and products. The species generation rate (θ_j) is obtained from the product between Eq. (8) and the third body effective concentration and can be estimated by:

$$\theta_j = \sum_{i=1}^{N} \alpha_{ij} \cdot C_i \cdot \gamma_j , \tag{9}$$

in which α_{ij} is the efficiency of chemical species i at a dissociation reaction j. Unfortunately, there is a lack of information about the efficiency of the molecules existent on a dissociation reaction model. Because of this, it is commonly adopted that the efficiencies of all chemical species are equal to unit and, in this case, the concentration of third body species corresponds to the whole number of existent species (Barros *et al*., 1990).

Table 1. Chemical reaction schemes implemented in software Mach1D 5.0.

Model	*L*	*N*	Species	Observations
0	0	3	H_2O, O_2, H_2	Ideal model
1	1	3	H_2O, O_2, H_2	–
2	2	4	H_2O, O_2, H_2, OH	–
3	4	6	H_2O, O_2, H_2, OH, O, H	4 reactions with 3rd body – Barros *et al*. (1990) and Smith *et al*. (1987)
4	4	6	H_2O, O_2, H_2, OH, O, H	4 reactions – Svehla (1964)
5	8	6	H_2O, O_2, H_2, OH, O, H	8 reactions (4 with 3rd body) – Barros *et al*. (1990)
7	8	6	H_2O, O_2, H_2, OH, O, H	8 reactions (4 with 3rd body) – Smith *et al*. (1987)
10	6	8	H_2O, O_2, H_2, OH, O, H, HO_2, H_2O_2	4 reactions from model 3 and 2 from Kee *et al*. (1990) – all the reactions including 3rd body
9	18	8	H_2O, O_2, H_2, OH, O, H, HO_2, H_2O_2	18 reactions (5 with 3rd body) – Kee *et al*. (1990)

The determination of mass generation rates is obtained by the product of Eq. (9) and molecular weight (M_i) of the species, resulting in

$$\dot{w}_i = M_i \sum_{j=1}^{L} \left(\Delta \nu_{ij} \cdot \theta_j \right), \tag{10}$$

where $\Delta \nu_{ij}$ is calculated by $\Delta \nu_{ij} = \nu''_{ij} - \nu'_{ij}$ and represents the difference between formed and consumed number of moles for a reaction j. For non-equilibrium model, mass generation rates determination is fundamental for the species conservation of mass. Equations (1) to (4) are enough for one-species, frozen and equilibrium flows mathematical formulation; for non-equilibrium flow, however, associated to these four equations must be taken into account the species continuity equation:

$$\frac{d}{dx}\left(\rho u S Y_i \right) = S \dot{w}_i , \tag{11}$$

which corresponds to the conservation of mass for each species separately.

2.2. Coolant flow

Only four equations are needed for the one-dimensional study of coolant flow through the entire regenerative cooling system of a thrust chamber: the mass conservation equation, the momentum conservation equation, the energy conservation equation and a polynomial constitutive relation for density:

$$\frac{d}{ds}\left(\rho_c u_c S_c \right) = 0 , \tag{12}$$

$$\frac{d}{ds}\left(\rho_c u_c S_c u_c \right) = -S_c \frac{dP_c}{ds} + F'_c , \tag{13}$$

$$c_{pc}\frac{d}{ds}\left(\rho_c\, u_c\, S_c\, T_c\right)=\beta\, T_c\, u_c\, S_c\,\frac{dP_c}{ds}+q_c', \tag{14}$$

$$\rho_c=\rho_1+\rho_2\, T_c+\rho_3\, T_c^2, \tag{15}$$

where: the index *c* corresponds to coolant properties; ρ, u, P and T are four dependent variables, related to density, velocity, pressure and temperature (respectively); s is the length of the flow along the center of a channel (Fig. 1); S_c is the internal cross-sectional area of coolant channels; F_c', β and q_c' are related to the viscous forces, volumetric thermal expansion coefficient and the heat loss to the coolant channel walls, in this order; and ρ_1, ρ_2 and ρ_3 are constants related to the chosen coolant.

2.3. Heat conduction through the wall

As reaction gas products have high temperature values, heat is transferred from them to thrust chamber walls by convection and radiation mechanisms. This energy is then conducted through walls to the coolant and transmitted to it by convection. The whole process can be modelled by:

$$q \;=\; (q_h''+q_r'')\,S_{wh} \;=\; q_w''\,S_{wh} \;=\; q_c''\,S_{wc}, \tag{16}$$

where: q is the heat transfer rate through the wall; S_{wh} is the internal wall area in contact with reaction gas products (Fig. 2); q_w'' is the heat flux through the wall; q_c'' is the heat flux to the coolant; and S_{wc} is the effective heat transfer area between the wall and the coolant.

More details about the employed mathematical model can be found in Marchi *et al*. (2000; 2004).

3. Numerical model

The mathematical models for reaction gas products and coolant flows (assembly to the heat conduction through the wall) in the thrust chamber structure are discretized using finite volume method. The domain is divided into *Nvol* control volumes, in axial directions x and s, in which the differential equations are integrated. For reaction gas products, a co-located grid arrangement, appropriated for all speed flows is used (Marchi and Maliska, 1994), associated with a second-order discritization scheme (CDS), with deferred correction (Ferziger and Perić, 2001); similar treatment is given to coolant flow model, except for the appliance for all speed flows, once the coolant flow is always subsonic. The systems of algebraic equations obtained are solved by TDMA method (Ferziger and Perić, 2001).

Pressure and velocity are coupled by SIMPLEC algorithm (Van Doormaal and Raithby, 1984), in order to convert the mass equation in a pressure (or better, in a pressure-correction) one. So, the mass conservation equation, Eq. (1) or Eq. (12), is used for determination of a pressure-correction (P'), while velocity (u) is obtained from the momentum equation, Eq. (2) or Eq. (13), and the energy equation, Eq. (3) or Eq. (14), is taken for temperature (T) determination. Density (ρ) is gotten from the state equation, Eq. (4), or from Eq. (15). Equation (11) is also needed for non-equilibrium flow. It must be noted that velocity (u) is evaluated from very reduced values (near null values) until supersonic ones, and not only for supersonic values, as commonly found in literature (Barros et al., 1990).

The iterative process for solving the reaction gas products mathematical model provided by Eqs. (1) to (4) or Eqs. (12) to (15) consists only on nine steps:

1. Definition of data (temperature, pressure, density, velocity) in an instant of time t.
2. Estimation of all variables in an instant t+Δt (time is used as a relaxation parameter).
3. Definition of thermophysical properties (such as the constant-pressure specific heat, Darcy friction factor and heat transfer coefficients by convection).
4. Coefficients calculation for the algebraic system (by discretization) of the momentum equation and solution of this system by TDMA for the velocity u.
5. Coefficients calculation for the algebraic system (by discretization) of the energy equation and solution by TDMA for temperature T.
6. Calculation of density ρ.
7. Coefficients calculation for the algebraic system (by discretization) of the mass equation and solution by TDMA for pressure correction P'.
8. Correction of ρ, P and u with P'.
9. Return to item 2, until the achievement of the desired number of iterations.

Over this basic algorithm, some modifications are necessary for reaction gas products flow, depending on the adopted physical model. For equilibrium and non-equilibrium models, step 3 includes also the chemical composition determination for all the domain control volumes and, also here, the determination of thermoproperties must be done for every single control volume. Non-equilibrium chemical composition determination includes, also, the use of Eq. (10), for mass generation rate evaluation, and Eq. (11), in order to estimate the chemical composition, respecting the mass conservation law for each species separately.

The adopted boundary conditions to reaction gas products flow include: definition of inlet temperature (T) and pressure (P) as functions of stagnation parameters (T_0 and P_0, in this order); the chemical mixture composition, given by mass fractions (Y_i), is obtained from local data (temperature and pressure); and the entrance velocity (u) is obtained from a linear extrapolation from the values obtained for internal flow. About exit conditions, for supersonic flows in nozzles, no exit boundary conditions are required; for the implementation of a numerical model, however, exit boundary conditions are needed. Because of this, temperature (T), velocity (u), pressure (P) and mass fractions (Y_i) are obtained by linear extrapolation from internal control volumes.

For coolant flow, some other boundary conditions are employed, as follows: for channels entrance, both temperature and velocity are fixed (T_{in} and u_{in}, in this order) and inlet pressure is obtained from linear extrapolation of values obtained for internal flow; for density, both inlet and outlet values are estimated by Eq. (15); exit pressure is defined as null and both, exit temperature and exit velocity, are obtained from linear extrapolation of values obtained for internal flow.

The coupling between reaction gas products and coolant flows is made by the heat conduction through the thrust chamber wall, according to the procedures presented by Marchi *et al*. (2004), which consists on seven steps:

1. First estimative of wall temperatures distribution, for the wall in contact with the reaction gas products.
2. Solution of reaction gas products flow.
3. Solution of coolant flow.
4. Evaluation of heat transfer rate between the reaction gas products and the coolant.
5. Evaluation of both wall temperatures: the temperature of the wall in contact with the reaction gas products and the wall in contact with the coolant.
6. Evaluation of heat transfer rate error, which consists on the difference between the reaction gas products-to-wall heat transfer rate and the wall-to-coolant heat transfer.
7. Return to item 2, until the achievement of the desired tolerance or the desired number of iterations.

4. Definition of the problem

The thrust chamber geometry used in this work is the same one presented by Marchi *et al*. (2000; 2004), which consists on a cylindrical section, called combustion chamber (with radius r_{in} and length L_C) assembled to a nozzle device, whose longitudinal section is defined by a cosine curve (with throat nozzle radius r_g and length L_n). The radius r, for $x > L_C$, is evaluated by the following equation:

$$r = r_g + \frac{(r_{in} - r_g)}{2}\left\{1 + \cos\left[2\pi\frac{(x - Lc)}{Ln}\right]\right\}, \tag{17}$$

where x corresponds to the position where the radius is evaluated. Despite the cylindrical section is called combustion chamber, it does not correspond to a real combustion chamber; the effects of fuel and oxidant injection, mixture and burning are not considered. Figure 3 shows all geometrical parameters of the thrust chamber studied in this work.

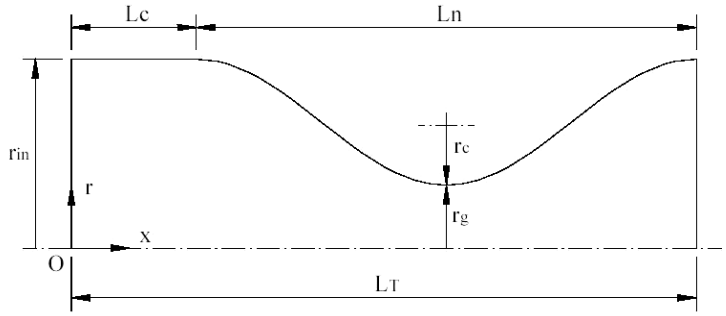

Figure 3. Geometrical parameters of the thrust chamber engine.

About the cooling system, the number of channels (m) placed around thrust chamber structure. The parameters, which define the geometrically the channels (Fig. 2) are: the thickness (e) of thrust chamber internal wall; the thickness

(t) of wall that separates two neighbour cooling channels; and the channels height (b). The average width of each channel ($\bar{a}$) is obtained as a function of previous parameters by

$$\bar{a} = \frac{\pi}{mb}\left[(r+e+b)^2 - (r+e)^2\right] - t, \tag{18}$$

when $m > 1$. While the parameters b, e and t remain constant, $\bar{a}$ does not have the same behaviour, due to radius variations.

Copper-made channels cover all the length of the thrust chamber engine, accompanying the variable radius of the engine. And, while the reaction gas products flows along the x-axis in a positive direction, the coolant flows in counter flow, namely, in s-axis negative direction. For all the studies presented in this work, the values used for geometrical parameters are: r_g = 0.1 m; r_{in} = 0.3 m; L_C = 0.1 m; L_n = 0.4 m; m = 200; b = 5.0 mm; e = 2.0 mm; and t = 1.5 mm. Based on these data, the ratio between the height and the average width of each channel ($b / \bar{a}$) varies between 0.62 and 2.8; the engine internal wall area is ≈ 9.242x10^{-1} m^2; the base channel area in contact with the coolant is ≈ 7.272x10^{-1} m^2 and the fins surface in contact with the coolant is ≈ 1.371 m^2. Water is taken as coolant and its mass flow rate is 1 kg/s in each channel, totalising 200 kg/s, with an inlet temperature of 300 K. Inside the combustion chamber, the stagnation temperature (T_0) is taken as 3420.33 K, while the stagnation pressure value (P_0) is 20 MPa and liquid oxygen and liquid hydrogen are injected at the stoichiometric composition (OF = 7.936682739). For isentropic analytical solution, the gas constant (R) is taken as 526.97 J/kg·K and the ratio between specific heats (γ) is 1.1956.

The aim of numerical solutions is given by the evaluation of some parameters of interest, cited in the following:

1. Nozzle discharge coefficient (C_d): defined as the ratio between numerical mass flux ($\dot{m}_{\text{num}}$) and the theoretical one ($\dot{m}_{\text{th}}$), obtained from isentropic analytical solution:

$$C_d = \frac{\dot{m}_{\text{num}}}{\dot{m}_{\text{th}}}. \tag{19}$$

2. Non-dimensional momentum thrust (F*): defined by the ratio between numerical and theoretical thrusts (F_{num} and F_{th}, in this order), given by

$$F^* = \frac{F_{\text{num}}}{F_{\text{th}}}, \tag{20}$$

where F corresponds to the thrust values and can be obtained by the following relation between mass flux ($\dot{m}$) and exit velocity (u_{ex}):

$$F = \dot{m} \cdot u_{ex}. \tag{21}$$

3. Pressure (P_{ex}), temperature (T_{ex}), velocity (u_{ex}) and Mach's number (M_{ex}) for gas products, at the nozzle exit.
4. Maximum wall temperature (T_{max}): obtained by wall temperature distribution.
5. Coolant pressure drop (ΔP): evaluated from channels entrance to its exit.
6. Exit coolant temperature (T_{cool}).

5. Numerical results and discussion

Four different physical models, including heat transfer effects, are studied in this work: a one-species gas with variable properties; a frozen gases mixture flow; an equilibrium gases mixture flow; and non-equilibrium gases mixture flow. All the analyses results were obtained employing a PC, with Pentium IV 3.4 GHz processor, 4 GB RAM, Windows XP. The results are then compared with those ones obtained by the same physical models (provided by both Mach1D 5.0 and CEA, this last one a numerical software provided by NASA), but without coolant flow effects (adiabatic walls).

For all the studies, the simulations were made for 3 different grids, to allow the determination of apparent and effective convergence orders (Marchi and Silva, 2002). Numerical error estimates, also, based on GCI estimator (Roache, 1994), were taken for all the physical and chemical models. Some pieces of information about numerical errors and error estimators can be found in Tannehill et al. (1997), Marchi (2001), and Ferziger and Perić (2001). Error estimates are very important for evaluating if two different physical (or chemical) models have the same results or the differences can be assigned to numerical errors. The GCI estimator is evaluated by

$$GCI(\varphi_1, p) = 3\frac{|\varphi_1 - \varphi_2|}{(q^p - 1)}, \tag{22}$$

where: φ_1 and φ_2 are, respectively, the numerical solutions for the refined (h_1) and coarse (h_2) grids; q is the grid refinement ratio ($q = h_2 / h_1$); h is the grid spacing or distance between two successive grid points; and p is related to the asymptotic (p_L) or apparent (p_U) order (the lowest value between the two ones). Asymptotic error order depends on the chosen discretization model, while apparent error, for constant refinement ratio, is evaluated by

$$p_U(h_1) = \frac{\log\left(\frac{\varphi_2 - \varphi_3}{\varphi_1 - \varphi_2}\right)}{\log(q)}, \tag{23}$$

where φ_3 corresponds to the numerical solution for a supercoarse grid.

Although nine chemical schemes are available at RHG1D 3.0 software for frozen and equilibrium flows and another six schemes are implemented for non-equilibrium flow, only models 3 and 10 (with six and eight species, respectively) for frozen and equilibrium flows and models 31 and 32 (both with six species) for non-equilibrium flow are studied in this work. According to results obtained by Marchi *et al*. (2005) and Araki and Marchi (2006), six and eight-species models present good accuracy with CEA results; because of this, only six and eight-species models results are reported in this work. Tables 2, 3 and 4 present the results for the variables of interest, including numerical error estimates, for an 80-volumes grid. The reason for using such a grid is based on other studies (Marchi *et al*., 2004; Araki and Marchi, 2006), for which numerical error estimates are about the same magnitude of experimental error; besides, CPU time consumption for an 80-volumes grid is much lower than the one required for a 10240 control volumes, or even a 2560 one (Araki and Marchi, 2006).

As can be seen from Table 2 results, heat transfer effects are not important for non-dimensional momentum thrust determination: there is no modification on values, when the simulations including or not such effects are compared. For nozzle discharge coefficient, there is a tiny variation on values, which can be bigger than the error estimates (like for frozen flow), however, which is no greater than 1%. Larger differences are observed (Tables 2 and 3) for local variables of interest, such as exit pressure, temperature and velocity. The heat transfer effects assembled to the chemical reactive flow provides a reduction on exit pressure, exit temperature and exit velocity values. This drop is about 400-750 Pa for exit pressure (which is equal, at maximum, to a reduction of 2.6%), 35-70 K for exit temperature (at maximum, a 4.5% reduction) and 15-35 m/s for exit velocity (at maximum, a 1.0% reduction). Such variations are motivated by the heat conduction to the coolant: once this energy is transferred, the temperature of the reaction gas mixture drops and, consequently, all the other thermophysical parameters are affected, including the chemical composition (for equilibrium and non-equilibrium models), as can be seen at Table 5.

Table 2. Comparison for C_d, F^* and P_{ex} (80 control volumes).

Results without heat transfer effects			
Model	**C_d [adim.]**	**F^* [adim.]**	**P_{ex} [Pa]**
Analytical (R1)	**1.0**	**1.0**	**2.917342×10^4**
One-species, variable Properties (R2)	$1.060 \pm 3 \times 10^{-3}$	$1.004 \pm 4 \times 10^{-3}$	$3.005 \times 10^4 \pm 4 \times 10^1$
Frozen Flow – mod. 3, 4, 5 and 7	$1.001 \pm 3 \times 10^{-3}$	$1.000 \pm 4 \times 10^{-3}$	$2.74 \times 10^4 \pm 1 \times 10^2$
Frozen Flow – mod. 9 and 10	$1.001 \pm 3 \times 10^{-3}$	$1.000 \pm 4 \times 10^{-3}$	$2.74 \times 10^4 \pm 1 \times 10^2$
CEA (frozen flow)	**1.000580**	**0.998992**	**2.7448×10^4**
Equilibrium Flow – mod. 3, 4, 5 and 7	$0.98 \pm 1 \times 10^{-2}$	$1.01 \pm 1 \times 10^{-2}$	$3.63 \times 10^4 \pm 5 \times 10^2$
Equilibrium Flow – mod. 9 and 10	$0.98 \pm 1 \times 10^{-2}$	$1.01 \pm 1 \times 10^{-2}$	$3.63 \times 10^4 \pm 5 \times 10^2$
CEA (local equilibrium flow)	**0.977372**	**1.011553**	**3.6178×10^4**
Non-equilibrium Flow – mod. 31	$1.008 \pm 3 \times 10^{-3}$	$1.012 \pm 5 \times 10^{-3}$	$3.175 \times 10^4 \pm 7 \times 10^1$
Non-equilibrium Flow – mod. 32	$1.007 \pm 3 \times 10^{-3}$	$1.014 \pm 5 \times 10^{-3}$	$3.254 \times 10^4 \pm 6 \times 10^1$
Results taking into account heat transfer effects			
Model	**C_d [adim.]**	**F^* [adim.]**	**P_{ex} [Pa]**
One-species, variable Properties (R2)	$1.070 \pm 3 \times 10^{-3}$	$1.004 \pm 4 \times 10^{-3}$	$2.942 \times 10^4 \pm 8 \times 10^1$
Frozen Flow – mod. 3	$1.011 \pm 3 \times 10^{-3}$	$0.999 \pm 4 \times 10^{-3}$	$2.67 \times 10^4 \pm 1 \times 10^2$
Frozen Flow – mod. 10	$1.011 \pm 3 \times 10^{-3}$	$0.999 \pm 4 \times 10^{-3}$	$2.67 \times 10^4 \pm 1 \times 10^2$
Equilibrium Flow – mod. 3	$0.98 \pm 1 \times 10^{-2}$	$1.01 \pm 1 \times 10^{-2}$	$3.59 \times 10^4 \pm 5 \times 10^2$
Equilibrium Flow – mod. 10	$0.98 \pm 1 \times 10^{-2}$	$1.01 \pm 1 \times 10^{-2}$	$3.59 \times 10^4 \pm 5 \times 10^2$
Non-equilibrium Flow – mod. 31	$1.012 \pm 3 \times 10^{-3}$	$1.012 \pm 5 \times 10^{-3}$	$3.10 \times 10^4 \pm 2 \times 10^2$
Non-equilibrium Flow – mod. 32	$1.011 \pm 3 \times 10^{-3}$	$1.013 \pm 3 \times 10^{-3}$	$3.18 \times 10^4 \pm 2 \times 10^2$

(R1): Rg = 526.97 J/kg·K; (R2): Rg ≈ 461.53 J/kg·K (equivalent to combustion gases mixture for the ideal model)

Table 4 provides the numerical results for coolant properties (as well as for heat transfer parameters). As can be seen, numerical results are quite independent from the physical model choice; even for exit coolant temperature, for

which the results are different (based on numerical error estimates), the maximum difference among models is only 0.54 K. Larger differences are found for the maximum heat flux (q_{max}) (from the reaction gas products to the coolant): it achieves 8.3×10^5 W/m^2 (comparing the one-species gas and frozen flow models); the effect of such variation on the maximum wall temperature, however, is quite small: only 8.5 K (for the same physical models) and, if frozen and equilibrium results are compared, this difference is even smaller: 5.5 K. Based on these results and on CPU time consumption, which is presented at Table 6, for coolant and wall properties definition, the frozen flow model is a good choice (even for an initial analysis): its results are quite the same of the other physical models and its CPU time consumption is the lowest one (even smaller than the monogas with variable properties).

Table 3. Comparison for T_{ex}, u_{ex} and M_{ex} (80 control volumes).

Results without heat transfer effects			
Model	T_{ex} **[K]**	u_{ex} **[m/s]**	M_{ex} **[adim.]**
Analytical (R1)	**1712.7409**	**3316.7150**	**3.1928346**
One-species, variable Properties (R2)	1800 ± 7	3142 ± 6	$3.15 \pm 1 \times 10^{-2}$
Frozen Flow – mod. 3, 4, 5 and 7	1606 ± 9	3312 ± 7	$3.24 \pm 1 \times 10^{-2}$
Frozen Flow – mod. 9	1606 ± 9	3312 ± 7	$3.24 \pm 1 \times 10^{-2}$
CEA (frozen flow)	**1607.91**	**3311.4519**	**3.231**
Equilibrium Flow – mod. 3, 4, 5 and 7	$2461.2 \pm 3 \times 10^{-1}$	3427 ± 2	$2.911 \pm 2 \times 10^{-3}$
Equilibrium Flow – mod. 9 and 10	$2461.4 \pm 3 \times 10^{-1}$	3427 ± 2	$2.911 \pm 2 \times 10^{-3}$
CEA (local equilibrium flow)	**2462.41**	**3432.7056**	**2.986**
Non-equilibrium Flow – mod. 31	$1910 \pm 1 \times 10^{1}$	3332 ± 6	$3.05 \pm 1 \times 10^{-2}$
Non-equilibrium Flow – mod. 32	$1980 \pm 1 \times 10^{1}$	3338 ± 6	$3.02 \pm 1 \times 10^{-2}$
Results taking into account heat transfer effects			
Model	T_{ex} **[K]**	u_{ex} **[m/s]**	M_{ex} **[adim.]**
One-species, variable Properties (R2)	1730 ± 7	3112 ± 6	$3.18 \pm 1 \times 10^{-2}$
Frozen Flow – mod. 3	1534 ± 9	3278 ± 7	$3.27 \pm 2 \times 10^{-2}$
Frozen Flow – mod. 10	1534 ± 9	3278 ± 7	$3.27 \pm 2 \times 10^{-2}$
Equilibrium Flow – mod. 3	$2425.4 \pm 8 \times 10^{-1}$	3409 ± 2	$2.922 \pm 2 \times 10^{-3}$
Equilibrium Flow – mod. 10	$2425.6 \pm 8 \times 10^{-1}$	3409 ± 2	$2.922 \pm 2 \times 10^{-3}$
Non-equilibrium Flow – mod. 31	$1860 \pm 1 \times 10^{1}$	3315 ± 6	$3.08 \pm 1 \times 10^{-2}$
Non-equilibrium Flow – mod. 32	1924 ± 9	$3320 \pm 2 \times 10^{1}$	$3.05 \pm 1 \times 10^{-2}$

(R1): $R_g = 526.97$ J/kg·K; (R2): $R_g \approx 461.53$ J/kg·K (equivalent to combustion gases mixture for the ideal model)

Table 4. Comparison for ΔP, T_{cool}, q_{max} and T_{max} with heat transfer effects (80 control volumes).

Model	ΔP **[Pa]**	T_{cool} **[K]**	q_{max} **[W/m^2]**	T_{max} **[K]**
One-species, variable Properties (R2)	$8.4 \times 10^5 \pm 3 \times 10^4$	$311.36 \pm 2 \times 10^{-2}$	$3.197 \times 10^7 \pm 5 \times 10^4$	$620.0 \pm 3 \times 10^{-1}$
Frozen Flow – mod. 3	$8.4 \times 10^5 \pm 3 \times 10^4$	$311.6 \pm 2 \times 10^{-1}$	$3.28 \times 10^7 \pm 1 \times 10^5$	$628.5 \pm 7 \times 10^{-1}$
Frozen Flow – mod. 10	$8.4 \times 10^5 \pm 3 \times 10^4$	$311.6 \pm 2 \times 10^{-1}$	$3.28 \times 10^7 \pm 1 \times 10^5$	$628.5 \pm 7 \times 10^{-1}$
Equilibrium Flow – mod. 3	$8.4 \times 10^5 \pm 3 \times 10^4$	$311.9 \pm 2 \times 10^{-1}$	$3.23 \times 10^7 \pm 4 \times 10^5$	623 ± 3
Equilibrium Flow – mod. 10	$8.4 \times 10^5 \pm 3 \times 10^4$	$311.9 \pm 2 \times 10^{-1}$	$3.23 \times 10^7 \pm 4 \times 10^5$	623 ± 3
Non-equilibrium Flow – mod. 31	$8.4 \times 10^5 \pm 3 \times 10^4$	$311.40 \pm 2 \times 10^{-2}$	$3.235 \times 10^7 \pm 9 \times 10^4$	$624.0 \pm 4 \times 10^{-1}$
Non-equilibrium Flow – mod 32	$8.4 \times 10^5 \pm 3 \times 10^4$	$311.46 \pm 2 \times 10^{-2}$	$3.240 \times 10^7 \pm 9 \times 10^4$	$624.5 \pm 4 \times 10^{-1}$

(R2): $R_g \approx 461.53$ J/kg·K (equivalent to combustion gases mixture for the ideal model)

Table 5. Reaction gas products composition at nozzle engine exit (80 control volumes).

Model		H_2O	O_2	H_2	OH	O	H	HO_2	H_2O_2	O_3
Frozen Flow, without heat transfer effects	3	0.78369	0.07754	0.01565	0.10276	0.01790	0.00247	---	---	---
	10	0.78354	0.07743	0.01565	0.10272	0.01789	0.00247	0.00027	0.00004	---
	CEA	**0.77987**	**0.07515**	**0.01570**	**0.10900**	**0.01751**	**0.00246**	**0.00027**	**0.00004**	**<0.00001**
Equilibrium Flow, without heat transfer effects	3	0.92742	0.03659	0.00606	0.02687	0.00259	0.00047	---	---	---
	10	0.92736	0.03661	0.00606	0.02689	0.00260	0.00047	0.00001	9.79×10^{-7}	---
	CEA	**0.92548**	**0.03579**	**0.00611**	**0.02956**	**0.00257**	**0.00047**	**0.00001**	**<0.00001**	**<0.00001**
Non-equilibrium Flow, without heat transfer effects	31	0.81253	0.10023	0.01709	0.05351	0.01592	0.00072	---	---	---
	32	0.82375	0.09475	0.01600	0.05132	0.01349	0.00068	---	---	---
Frozen flow, taking into account heat transfer effects	3	0.78369	0.07754	0.01565	0.10276	0.01790	0.00247	---	---	---
	10	0.78354	0.07743	0.01565	0.10272	0.01789	0.00247	0.00027	0.00004	---
Equilibrium flow, taking into account heat transfer effects	3	0.93600	0.03279	0.00540	0.02339	0.00205	0.00038	---	---	---
	10	0.93595	0.03281	0.00540	0.02340	0.00205	0.00038	0.00001	<0.00001	---
Non-equilibrium flow, taking into account heat transfer effects	31	0.81681	0.09883	0.01680	0.05189	0.01504	0.00062	---	---	---
	32	0.82832	0.09342	0.01570	0.04929	0.01269	0.00059	---	---	---

Table 6. CPU time physical models; simulations including heat transfer effects (80 control volumes).

Model		Iterations for:		Global iterations	CPU time
Physical	Chemical	Reaction products flow	Coolant flow		
Monogas, variable properties	**---**	6,000	1,000	20	23.4 s
Frozen Flow	**3**	5,000	1,000	20	10.6 s
	10	5,000	1,000	20	12.2 s
Equilibrium Flow	**3**	15,000	1,000	20	1.79 h
	10	15,000	1,000	20	3.49 h
Non-Equilibrium Flow	**31**	5,000,000	1,000	5	1.06 day
	32	4,000,000	1,000	5	20.0 h

From Table 5, it can be noted that the reaction gas products compositions, for both equilibrium and non-equilibrium flows, taking into account heat transfer effects, are only a little different from those obtained for adiabatic walls. It is related to the small drop at the temperature profile through the entire nozzle engine, considering heat transfer effects, as can be seen at Fig. 4. The lower the temperature, the smaller the species dissociation effects; because of this, all the species mass fractions drop when the heat transfer effects are considered, but the H_2O one.

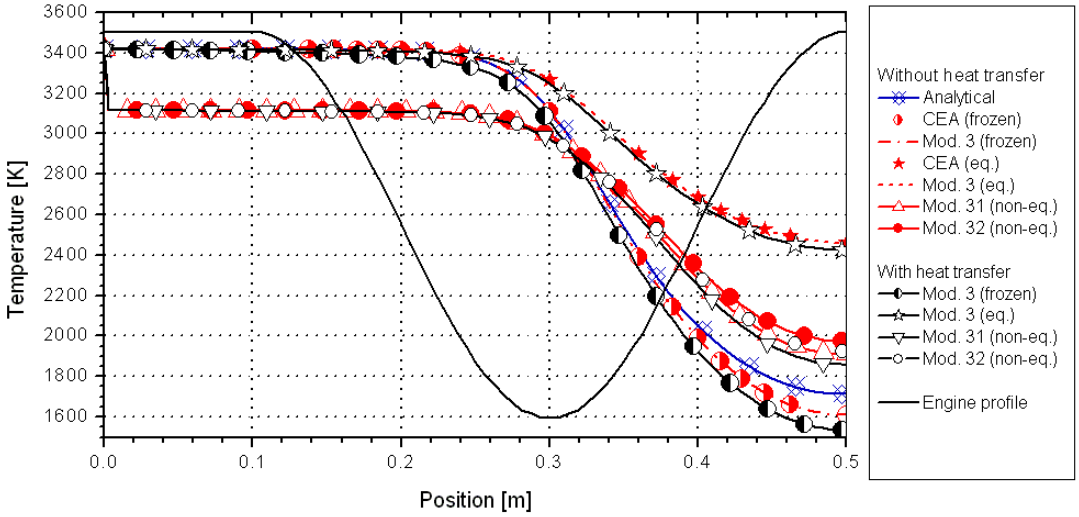

Figure 4. Temperature distribution of reaction gas products through the nozzle engine.

Beside the CPU time consumption for physical and chemical models studied in this work, Table 6 provides the number of iterations for solving each problem (reaction gas products and coolant flows) separately and, also, the number of global iterations. These amounts of iterations were chosen in order to allow the convergence of each sub-problem separately (reaction gas products and coolant flows), at each global iteration. The number of total global iterations was chosen in order to achieve the round-off error (except for non-equilibrium flow, for which a tolerance of 10^{-5} was specified). This proceeding was necessary to minimize other types of numerical errors than discretization ones and, in this way, to guarantee that numerical errors are made, essentially, of discretization ones.

While Fig. 4 presents the temperature distribution of reaction gas products through the nozzle engine, Fig. 5 provides the wall temperature (in contact with reaction gas products) along the whole engine. Despite the differences on temperature values at thrust chamber entrance and exit, all the physical models have similar solutions for maximum wall temperature (actually, the difference at numerical results is smaller than 10K, as previously commented).

Although frozen flow presents lower temperatures for reaction gas products than equilibrium flow ones, wall temperatures are, at least from thrust chamber entrance to nozzle throat, higher than those obtained for equilibrium flow studies. This phenomenon is explained by the higher values for convection heat transfer coefficient verified for frozen flow, which achieves, at maximum, 11,691 $W/m^2 \cdot K$ at nozzle throat region (against 10,861 $W/m^2 \cdot K$ for equilibrium flow model). Thus, even though the recombination reactions, which take place along all the thrust chamber length and forms H_2O species, are exothermic and contribute to the higher reaction gas products temperatures, the higher values for convection heat transfer coefficient, verified for frozen flow model, overtake these recombination effects and its associated higher temperature, at least until nozzle throat region, where the highest wall temperatures are found. Otherwise, the difference between frozen flow and equilibrium flow reaction gas temperatures after the nozzle throat region becomes so expressive that the effects of the higher values for convection heat transfer coefficient (verified for frozen flow model) are overtaken by the higher equilibrium flow temperature values for reaction gas products. Because of this, the wall temperatures, from the nozzle throat to the thrust chamber exit, are higher for the equilibrium flow model.

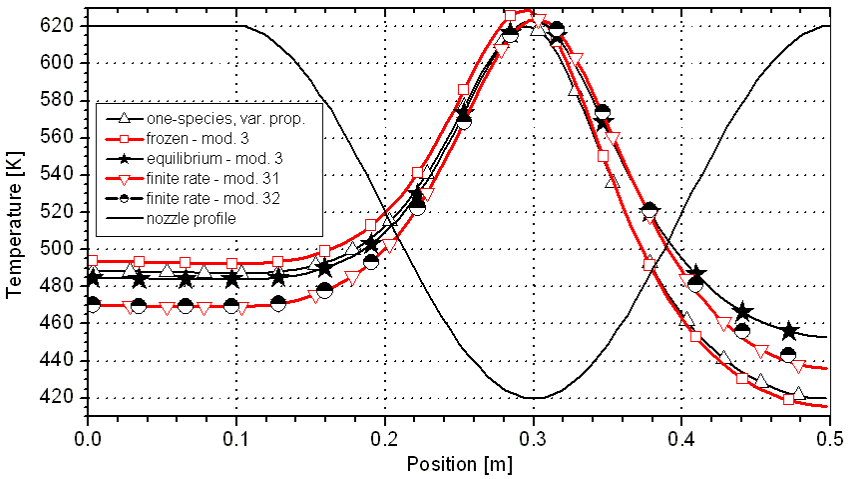

Figure 5. Wall temperature distribution (in contact with reaction gas products) through the nozzle engine.

6. Conclusion

A software for one-dimensional chemical reactive flow with regenerative cooling was implemented, using FORTRAN 95 language and Visual Compaq 6.6.0 compiler. Four physical models were studied: a one-species flow (with variable properties); and the other three for reaction gas products (frozen, local equilibrium and non-equilibrium flows). For frozen and equilibrium models, nine different chemical reaction schemes were implemented, the same chemical reaction schemes discussed by Marchi et al. (2005), but only two were studied (a six and a eight-species models) and the results were compared to those ones obtained for adiabatic wall studies, including those ones from the NASA's software CEA. For non-equilibrium, only six and eight-species reaction schemes were employed, totalising six models, comparing the results to frozen and local equilibrium ones. Unfortunately, because of time restrictions, only two from these six models were studied.

Differently as usually found in literature, the energy equation has the temperature as unknown (and not the enthalpy nor the internal energy, as commonly used). The major advantage of such variation is about the temperature determination, which is done directly from the numerical model. Also, the velocity determination is done from the combustion chamber (where the velocity is almost null) to the nozzle exit (supersonic flow), covering all the velocity regimes in a real engine (subsonic, transonic and supersonic ones), and not only the supersonic flow, as commonly done.

Assembling refrigeration effects to reaction gas products flow has only small influence on global parameters of interest: for nozzle discharge coefficient, there is only a tiny variation on values, which can be bigger than the error estimates (like for frozen flow), however, which is no greater than 1%; for non-dimensional momentum thrust, no appreciable variation on numerical results was verified. For local parameters of interest, otherwise, larger differences were observed, especially for exit temperature values, for which a drop between 35 and 70 K at exit temperature (at maximum, a 4.5% reduction, for frozen flow model) was verified. At exit velocity and exit pressure, such variations are smaller: only a 1.0% reduction for velocity (15-35 m/s) and a 2.6% reduction for pressure (about 400-750 Pa). The reaction gas products compositions, for both equilibrium and non-equilibrium flows, taking into account heat transfer effects, are only a little different from those obtained for adiabatic walls.

Comparing the physical models results for coolant parameters of interest, it was observed only a small variation on coolant exit temperature: 0.54 K, while the pressure drop values are the same for all the models studied. For maximum heat flux (from the reaction gas products to the coolant), the difference more expressive: it achieves 8.3×10^5 W/m^2 (comparing the one-species gas and frozen flow models); the effect of such variation on the maximum wall temperature, however, is quite small: only 8.5 K (for the same physical models).

Frozen flow model presents higher values for wall temperatures from thrust chamber entrance until its throat region, although equilibrium flow model shows greater reaction gas products temperatures. This phenomenon is consequence of the higher values for convection heat transfer coefficient verified for frozen flow model and, because of this, the highest value for maximum wall temperature was 628.5 K, for frozen flow model. From the nozzle throat region to the exit thrust chamber, the effects of the higher values for convection heat transfer coefficient are overtaken by those ones caused by the greater reaction gas products temperature, what explains the higher wall temperature values for equilibrium flow after the nozzle throat region.

For all the studies, 80-volumes grids were employed, once they provide numerical error estimates at the same magnitude of experimental ones (Marchi *et al*., 2004; Araki and Marchi, 2006). Comparing numerical results (for coolant and wall properties definition) and also CPU time requirements, the frozen flow model is a good choice (even for an initial analysis): its results are quite the same of the other physical models and its CPU time consumption is the

lowest one (even smaller than the monogas with variable properties, which demands at least 90% more time): it is at least more than 500 times faster than the equilibrium flow model and 5500 times faster the than non-equilibrium one.

7. Acknowledgement

The authors would acknowledge Federal University of Paraná (UFPR), Coordenação de Aperfeiçoamento de Pessoal de Nível Superior (CAPES) and The "UNIESPAÇO Program" of The Brazilian Space Agency (AEB) by physical and financial support given for this work. The first author would, also, acknowledge his professors and friends, by discussions and other forms of support.

8. References

Araki, L. K., Marchi, C. H., 2006, "Effects of Chemical Reaction Schemes and Physical Models on a One-Dimensional Flow in a Rocket Engine Nozzle", Proceedings of the 27th Iberian Latin-American Congress on Computational Methods in Engineering, Belém, Brazil. Paper CIL04-500. (Paper submitted.)

Barros, J. E. M., Alvim Filho, G. F., Paglione, P., 1990, "Estudo de Escoamento Reativo em Desequilíbrio Químico através de Bocais Convergente Divergente", Proceedings of the III Encontro Nacional de Ciências Térmicas, Itapema, Brazil.

Ferziger, J. H. and Perić, M., 2001, "Computational Methods for Fluid Dynamics", 3ed., Berlin: Springer-Verlag.

Fröhlich, A., Popp, M., Schmidt, G., Thelemann, D., 1993, "Heat Transfer Characteristics of H_2/O_2 Combustion Chambers", Proceedings of the 29th Joint Propulsion Conference, Monterrey, USA, AIAA 93-1826.

Glenn Research Center, 2005, "CEA – Chemical Equilibrium with Applications", available at: <http://www.grc.nasa.gov/WWW/CEA Web/ceaHome.htm>, access in: Feb 16, 2005.

Kee, R. J., GrCar, J. F., Smooke, M. D, Miller, J. A., 1990, "A Fortran Program for Modeling Steady Laminar One-Dimensional Premixed Flames", Albuquerque: Sandia National Laboratories, SAND85-8240•UC-401.

Marchi, C. H., 2001, "Verificação de Soluções Numéricas Unidimensionais em Dinâmica dos Fluidos", Thesis (Mechanical Engineering PhD). Universidade Federal de Santa Catarina, Florianópolis, SC.

Marchi, C. H., Araki, L. K., Laroca, F., 2005, "Evaluation of Thermochemical Properties and Combustion Temperatures for LOX/LH_2 Reaction Schemes", Proceedings of the 26th Iberian Latin-American Congress on Computational Methods in Engineering, Guarapari, Brazil. Paper CIL06-0095.

Marchi, C. H., Laroca, F., Silva, A. F. C., Hinckel, J. N., 2000, "Solução Numérica de Escoamentos em Motor-Foguete com Refrigeração Regenerativa", Proceedings of the 21st Iberian Latin-American Congress on Computational Methods in Engineering, Rio de Janeiro, Brazil.

Marchi, C. H., Laroca, F., Silva, A. F. C., Hinckel, J. N., 2004, "Numerical Solutions of Flows in Rocket Engines with Regenerative Cooling", Numerical Heat Transfer, *Part A*, Vol.45, pp. 699-717.

Marchi, C. H., Maliska, C. R., 1994, "A nonorthogonal finite volume method for the solution of all speed flows using co-located variables", Numerical Heat Transfer*, Part B*, v. 26, pp. 293 – 311.

Marchi, C. H., Silva, A. F. C., 2002, "Unidimensional numerical solution error estimation for convergent apparent order", Numerical Heat Transfer, *Part B*, Vol. 42, pp. 167-188.

Roache, P. J., 1994, "Persperctive: A method for uniform reporting of grid refinement studies", Journal of Fluids Engineering, Vol. 116, pp. 405-413.

Smith, T. A., Pavli, A. J., Kacynski, K. J., 1987, "Comparison of Theoretical and Experimental Thrust Performance of a 1030:1 Area Ratio Rocket Nozzle at a Chamber Pressure of 2413 kN/m^2 (350 psia)", Cleveland, NASA Lewis Research Center, NASA Technical Paper 2725.

Sutton, G. P., Biblarz, O, 2001, "Rocket Propulsion Elements", 7 ed., New York, John Willey & Sons.

Svehla, R. A., 1964, "Thermodynamic and Transport Properties for the Hydrogen-Oxygen System", Cleveland, NASA Lewis Center, NASA SP-3011.

Tannehill, J. C., Anderson, D., Pletcher, R. H., 1997, "Computational Fluid Mechanics and Heat Transfer", 2ed., Philadelphia: Taylor & Francis.

Van Doormal, J. P., Raithby, G. D., 1984, "Enhancements of the SIMPLE method for predicting incompressible fluid flow", Numerical Heat Transfer, v. 7, pp. 147-163.